Gold Bull (2011) 44:199–205
DOI 10.1007/s13404-011-0032-7

ORIGINAL PAPER

On the ultrathin gold film used as buffer layer at the transparent conductive anode/organic electron donor interface

L. Cattin · S. Tougaard · N. Stephant · S. Morsli · J. C. Bernède

Published online: 14 October 2011

Abstract Previously, we have shown that a gold thin film of only 0.5 nm introduced at the interface between the indium tin oxide or ZnO anode and the organic electron donor in organic photovoltaic cells induces a strong improvement of the cell efficiency. Of course a thickness of 0.5 nm corresponds only to an averaged thickness, the films being too thin to be continuous. For a clear understanding of the physical mechanisms that are responsible for this improved behaviour, it is important to know the fractional coverage and the island height of this thin Au film. In the present work, we have used two different techniques, such as treated scanning electron microscope images and analysis of the inelastic part of peaks of X-ray photoelectron spectroscopy spectra, to estimate the gold coverage and island height of the transparent conductive anode. There is an excellent agreement between the results achieved by both methods. Only 15% of the anode is covered, which proves the high efficiency of gold as an anode buffer layer in organic photovoltaic devices.

L. Cattin (✉) · N. Stephant
Université de Nantes, Institut Jean Rouxel (IMN),
UMR 6502, 2 rue de la Houssinière,
BP 92208, Nantes 44000, France
e-mail: linda.cattin-guenadez@univ-nantes.fr

S. Tougaard
Department of Physics and Chemistry,
University of Southern Denmark,
DK-5230 Odense M, Denmark

S. Morsli
Université de Nantes, LAMP,
2 rue de la Houssinière, BP 92208, Nantes 44000, France

J. C. Bernède
Université de Nantes, Moltech Anjou,
UMR 6200, 2 rue de la Houssinière
BP 92208, Nantes 44000, France

Keywords Organic solar cells · X-ray photoelectron spectroscopy · Scanning electron microscope

Introduction

Nowadays, organic photovoltaic cells (OPV) are the object of a very large scientific interest because, in the future, they could constitute an alternative to the current inorganic cells. New materials and original concepts have allowed achieving power conversion efficiencies (PCE) certified at more than 8% (http://www.heliatek.com). Much effort has been done for reaching 10%. One of the factors limiting the PCE is the carrier collection by the electrodes [1]. The carrier collection efficiency depends on a good energy alignment of the electrodes and the organic materials. Low-energy barriers for electron and hole collection are required for OPVs. With regard to holes, generally, an indium tin oxide (ITO) electrode is used as the hole extraction electrode in contact with the organic electron donor (OED). It is known that commercial ITO rarely presents good band matching with the OED. Many techniques have been proposed for the engineering of the interface ITO anode/OED, such as surface treatment by ozone plasma, deposition of a self-assembled monolayer and introduction of a buffer layer at the interface [2]. Among these techniques, a gold film of 1 nm thickness or more has been used to tailor the anode work function in optoelectronic devices [3–5]. We have shown that the deposition of an ultrathin gold film at the interface between the anode and the OED allows achieving PCE as high as those with the well-known poly(3,4-ethylenedioxythiophene) poly(styrenesulfonate) (PEDOT:PSS) [6]. Moreover, a similar PCE can be obtained whatever the transparent conductive oxide (TCO) used: aluminium-doped zinc oxide or fluorine-doped tin oxide [7]. Moreover, it should be noted that whilst the

thickness of the PEDOT:PSS buffer layer is around 50 nm, the optimum thickness of the gold buffer layer is only 0.5 nm, the thickness being measured by a quartz monitor. In that range of thickness, the value measured is averaged, the real films being discontinuous. In the present study, we used two techniques which allow estimating the rate of covering of the TCO film by the gold. The first one is based on scanning electron microscopy (SEM). A software is used to analyse the image so as to deduct the coverage and island height of the thin TCO film by the gold. The second approach is based on the analysis of the shape of the Au4d XPS peak. This method relies on the fact that the longer distance the photoelectron has travelled the more inelastic scattering events it has experienced. These inelastic scatterings move intensity from the XPS peak to lower energies, and as a result, the intensity and the shape of the peak in an energy range below the peak depend on the path length the photo-excited electrons have travelled in the solid before escaping through the solid surface. Proper analysis of the shape therefore allows determining the depth distribution of the Au atoms. For this analysis, specific software is used to deduce the coverage and height of the deposited gold. It is shown that both techniques give nearly identical experimental values, which shows the consistency of both techniques.

Experimental

The OPV multilayer cells were based on the couple copper phthalocyanise/fullerene (CuPc/C60). The TCO used were ITO and ZnO, whilst the cathode was an aluminium film. Two anode buffer layers have been used, either PEDOT:PSS or Au. The PEDOT:PSS layer was spin-coated onto the ITO anode from a 2.5% water solution. After spin coating, the PEDOT:PSS-covered anodes were annealed at around 100°C for 1 h to remove the solvent; its thickness was around 50 nm. The gold film, of thickness 0.5 or 1.5 nm, is introduced as the anode buffer layer in TCO/Au/CuPc/C60/BCP/Al classical OPV cells. The bathocuproine (BCP) layer, called the exciton blocking layer, improves significantly the performance of the OPV cells [8]. Except for PEDOT:PSS, all the films are deposited under vacuum. Before utilisation, the TCO-coated substrates were scrubbed with soap and then rinsed in running deionised water. Then, they were dried with an argon flow and loaded into a vacuum chamber (10^{-1} Pa). The thin film's deposition rates and thickness were estimated in situ with a quartz monitor after calibration using a field emission SEM (JEOL F-7600). The cross-sections of the films were visualized and then the films' thicknesses measured using simple software. The deposition rate and final thickness were 0.05 nm/s and 35 nm in the case of CuPc, 0.05 nm/s and 40 nm in the case of C_{60} and 0.1 and 9 nm for BCP. These thicknesses have been chosen after optimisation.

After organic thin film deposition, without breaking the vacuum, the aluminium top electrodes, through a mask with 2×8 mm active areas and then an approximately 100 nm encapsulating layer of amorphous selenium, were thermally evaporated [9]. After OPV deposition, electrical characterizations were performed with an automated *I–V* tester, in the dark and under sun global AM1.5 simulated solar illumination.

The morphology of the different structures used as anodes was observed through SEM with a JEOL 7600F at the 'Centre de Microcaractérisation de l'Université de Nantes'. Images in secondary and backscattering mode have been done. Because the average atomic number of gold is far from that of TCO atoms, the backscattering mode allowed us to obtain well-contrasted pictures for further treatment by ImageJ software. This last one was used to estimate the rate coverage of the TCO films by the gold nanodots [10]. Only the powerful resolution of this field emission SEM with its large-angle backscattered detector allowed us to obtain images at a very high magnification in backscattered mode.

X-ray photoelectron spectroscopy (XPS) measurements (Leybold LHS12, University of Nantes-CNRS) were performed to investigate the coverage and height of the structures formed by the deposited Au. The XPS spectra were acquired using a magnesium X-ray source (1,253.6 eV) operating at 10 kV and 10 mA. During the measurements, the vacuum was 10^{-7} Pa and the pass energy was 126 eV. The samples were ground with silver paste to prevent charge effect.

Experimental results

Influence of the different anode structures on the performance of the OPV cells

Before any experimental characterization of the different anodes, we have used them in classical OPV cells. The *J–V* characteristics are shown in Figs. 1 and 2, whilst the main parameters are presented in Table 1. It can be seen that the results achieved with the ultrathin gold film are similar, and even better than those obtained with the PEDOT:PSS. The optimum Au thickness is 0.5 nm. For thicker films, the short circuit current decreases, whilst the open circuit voltage (V_{oc}) and the fill factor (FF) are mostly stable. Therefore, the PCE decrease is due to J_{sc}, which varies in the same way as the transmission of light through the anode (Fig. 3). The higher efficiency obtained with 0.5 nm of Au, by comparison with that achieved with PEDOT:PSS, is

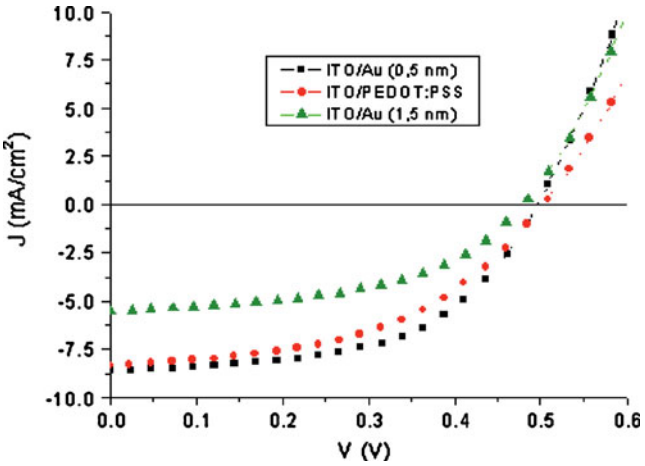

Fig. 1 *J–V* characteristics under AM1.5 illumination of solar cells with different anode configuration, ITO being the TCO

mainly due to FF improvement (Table 1). It is known that the FF value increases when the series resistance of the OPV cell decreases. Therefore, the variation of FF is due to the fact that the conductivity of Au is higher than that of PEDOT:PSS.

On the other hand, the PEDOT:PSS buffer layer, being 50 nm thick, covers continuously the ITO, as can be seen in Fig. 4, so it modifies the anode surface properties. As a matter of fact, it is known that the work function of PEDOT:PSS is 5.1 eV, whilst that of ITO is around 4.7 eV and the HOMO value of CuPc is 5.2 eV. Therefore, the improvement of the contact between ITO and OED, in the presence of PEDT:PSS, can be mainly attributed to a better band matching at the inorganic/organic interface. In the case of the Au buffer layer, if its work function is also 5.1 eV, its very small thickness (0.5 nm) makes its coverage of the ITO film more critical. For a better understanding of the functionality of the Au film, it is essential to know its coverage of the ITO film. Therefore, we have investigated

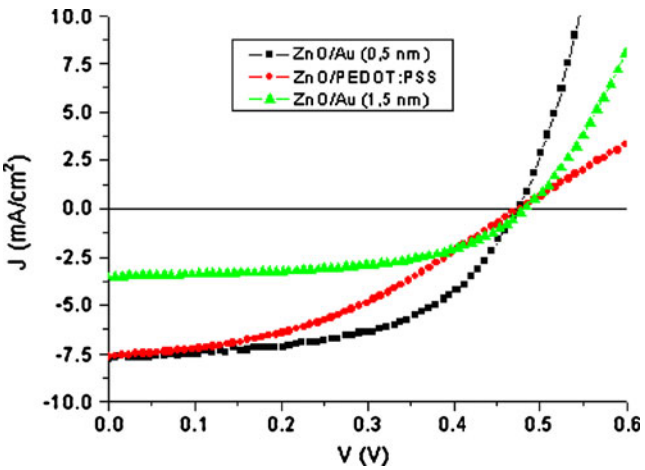

Fig. 2 *J–V* characteristics under AM1.5 illumination of solar cells with different anode configuration, ZnO being the TCO

Table 1 Photovoltaic characteristics, under light AM1.5 (100 mW cm^{-2}), for different cells using different anode configurations in devices based on the heterojunction CuPc/C_{60}

Anode	J_{sc} (mA/cm^2)	V_{oc} (V)	FF (%)	η (%)
ITO/PEDOT:PSS	8.30	0.50	49	2.02
ITO/Au 0.5 nm	8.60	0.50	54	2.32
ITO/Au 1.5 nm	5.50	0.48	50	1.33
ZnO/PEDOT:PSS	7.65	0.48	40	1.48
ZnO/Au 0.5 nm	7.70	0.48	55	2.01
ZnO/Au 1.5 nm	3.50	0.48	55	0.93

the fractional coverage and island heights of the gold buffer layer. To achieve this, we have performed a comparative study using two different techniques. The first one is based on the SEM images treated through ImageJ, an open-source software, and the second one is an indirect technique based on the analysis of the inelastic peak shape of the XPS photoemission spectra, which has been developed by Tougaard [11–14]; the algorithms have been implemented in the QUASES-Tougaard software package [15] which was used for the present analysis.

XPS and SEM experimental results analysis process

The experimental XPS and SEM results have been analysed using specific software. In the case of the SEM study, the pictures have been exploited using the open-source software ImageJ (http:/rsb.info.nih.gov/ij/). Such software allows improving the exploitation of the images themselves. SEM backscattered images were first filtered to reduce the noise and then converted to binary image by threshold operation to see the area covered by gold particles (in black) and that of the substrate (in white). Then, ImageJ

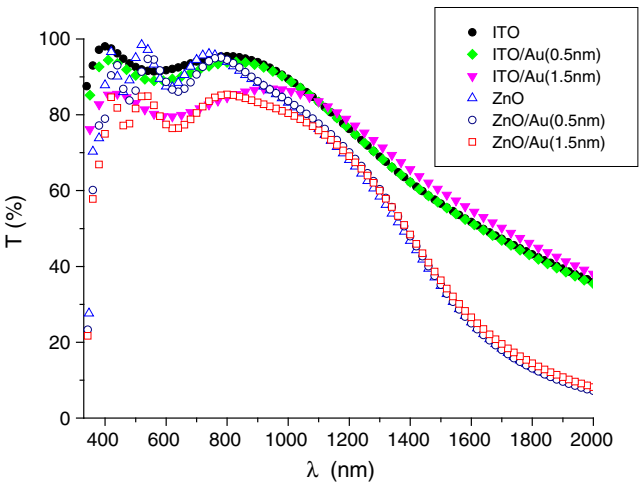

Fig. 3 Variation of the transmittance of TCO/Au structures with the Au thickness (0, 0.5 and 1.5 nm) and TCO (ITO-full symbols, and ZnO-open symbols)

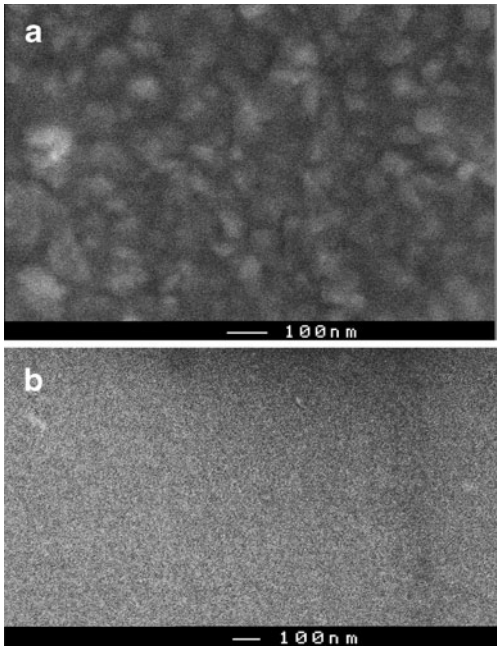

Fig. 4 Surface morphology of ITO (**a**) and Au/PEDOT:PSS superposed thin films (**b**)

can measure this covering [10]. The ITO example is shown in Fig. 5 (0.5 nm of Au) and in Fig. 6 (1.5 nm of Au). From Figs. 5 and 6, the first objective was to evaluate the rate of covering of the thin TCO film by the gold. To achieve this goal, we have looked for a higher contrast adjustment than usual when we took the backscattered images with the SEM to facilitate the ImageJ job (Figs. 5c and 6c). From the binary images, ImageJ can also calculate the average distance between nanodots through several steps. The same procedures have been used for the different samples, ITO and ZnO. The results of the different calculations are presented in Table 2.

Whilst the nanodot size increases significantly (from 5–7 to 19–20 nm^2) with the thickness of the deposited layer (0.5–1.5 nm), the average distance between nanodots only decreases slightly (from 6.5–6 to 5–4.8 nm), which means that there is coalescence of the nanodots. This result is in good agreement with the gold coverage, which increases with the gold thickness.

These results have been compared with those obtained by the analysis of the inelastic peak shape of the XPS photoemission spectra. For the ITO and ZnO samples with deposited Au, the XPS peak shape analysis can be done by an analysis of either the In and Zn(L3M45M45) Auger peak from the substrate, respectively, or it can be done from an analysis of the Au4d peak from the overlayer. Since we had easy access to record a reference spectrum from a pure gold foil, we have chosen to use the Au4d peak for the analysis. Examples of the XPS spectra of the Au4d peak region (after subtracting the intensity level measured on the high kinetic energy side of the peak) from a pure gold foil and from ITO films with nominally 0.5 and 1.5 nm gold are shown in Fig. 7. It can be clearly seen that both the shape and the intensity vary with the amount of Au deposited. The results, obtained from the analysis with the QUASES-Tougaard method of the two Au spectra, are shown in Figs. 8 and 9, respectively.

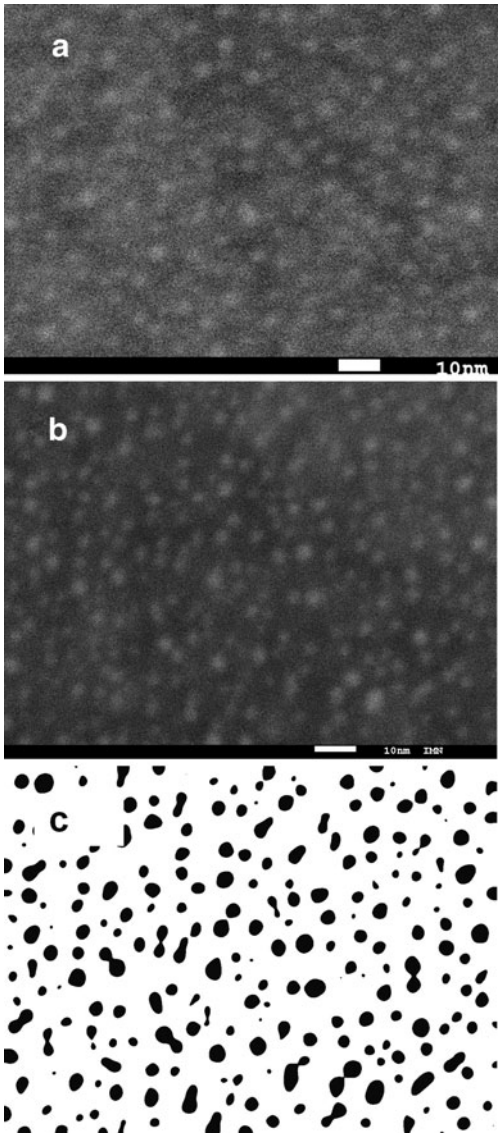

Fig. 5 SEM study of ITO/Au (0.5 nm). **a** Surface morphology. **b** Image in the backscattering mode. **c** Image treated with ImageJ

The analysis is done with the "analyze" part of the software which calculates the correction for inelastically scattered electrons corresponding to an assumed depth distribution of Au atoms. First, the spectrum from the pure Au foil is corrected using the knowledge that the Au atoms are homogeneously distributed in this sample. This gives a reference-corrected spectrum with which the other Au spectra should match both in intensity and in shape. In

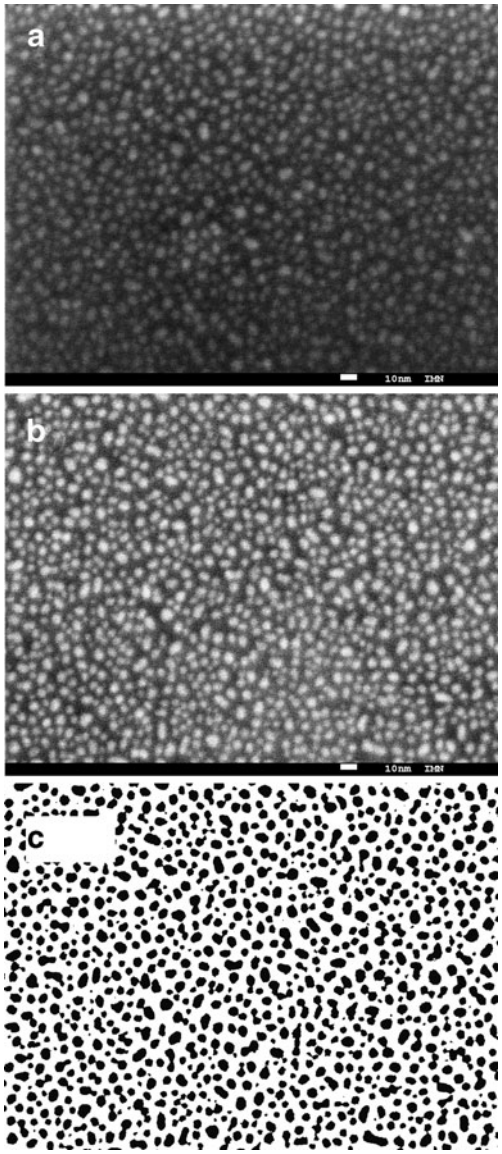

Fig. 6 SEM study of ITO/Au (1.5 nm). **a** Surface morphology. **b** Image in the backscattering mode. **c** Image treated with ImageJ

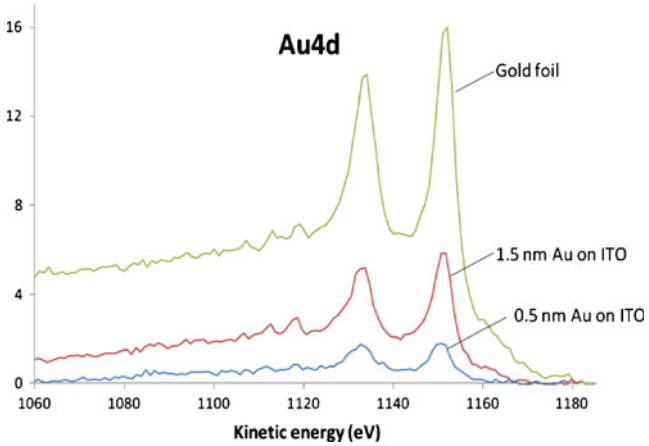

Fig. 7 XPS of the Au4d energy region from a pure gold foil and from ITO films with nominally 0.5- and 1.5-nm deposited Au

the upper panels of Figs. 8 and 9, it has been assumed that the Au forms a continuous layer and its thickness was varied until the intensity at the peak position is identical to the intensity of the reference spectrum at the main peak energy. As can be seen, the shapes of the corrected spectra are, however, very different from the reference Au4d spectrum. This tells us that the depth distribution is wrong.

In the lower panels of Figs. 8 and 9, the same two Au4d spectra have been corrected under variations of both the coverage and the height of the deposited Au. For the 0.5 nm sample, Fig. 8 clearly shows that with an island height of 2.4 nm and coverage of 16%, there is a very good agreement both in intensity and shape with the reference spectrum. A similar analysis of the 1.5 nm nominal thick gold layer is shown in Fig. 9, and it is seen that the shape and the intensity give a good match with the reference for islands of 4.2 nm height and 40% coverage. These structural parameters are also shown in Table 2. Note that the total amounts of Au in the islands are 0.16× 2.4 nm=0.384 nm and 0.4×4.2 nm=1.68 nm, respectively. These numbers are close to the nominal depositions of 0.5 and 1.5 nm.

The distance between the formed nanoparticles on the surface cannot be determined with the QUASES-Tougaard XPS peak shape analysis method. However, if we assume

Table 2 Gold coverage of the transparent conductive anodes estimated using treated scanning electron microscope images and inelastic peaks of X-ray photoelectron spectroscopy spectra

Substrate	Gold thickness (nm)	Gold coverage (%)		Average nanodot size (nm^2)		Other SEM results
		XPS	SEM	XPS	SEM	Averaged distance between nanodots (nm)
ITO	0.5	16	17.0	5.8	7.5	6
	1.5	40	32.5	17.6	20.0	4.8
ZnO	0.5	14	13.5	4.8	5.5	6.4
	1.5	(36)	32	(19.4)	19.0	5

The XPS analysis for 1.5 nm on ZnO is shown in parenthesis because it is uncertain due to the presence of Ag peaks originating from the silver paste in the XPS spectrum for this sample

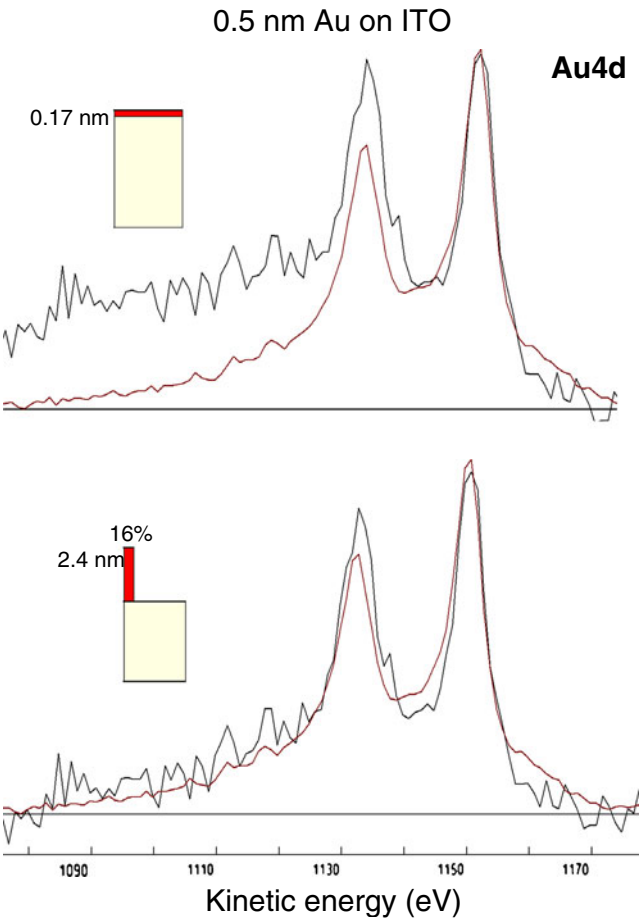

Fig. 8 The *lower spectrum in the upper panel* is the Au4d spectrum from the pure gold foil after correction for the inelastically scattered electrons. This must be compared on an absolute scale with the corrected Au4d spectra of the Au-deposited samples. In the *upper panel*, it is compared with the Au4d spectrum from the 0.5-nm Au on ITO after correction for inelastically scattered electrons assuming a continuous layer 0.17 nm thick. This thickness was chosen to make it match with the intensity of the reference Au4d spectrum at the peak energy. As can be seen, the disagreement is very large for energies below the peak energy. A perfect match is, however, obtained with respect to both intensity and shape with 16% coverage and 2.4-nm average height (shown in the *lower panel*)

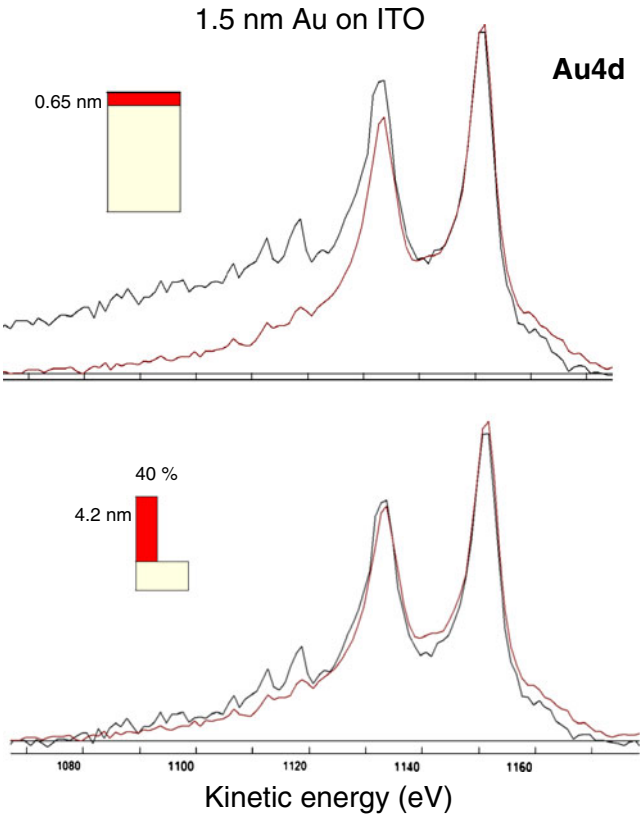

Fig. 9 Same as Fig. 8, but for the 1.5-nm Au on ITO sample

that the Au islands form spheres (which is likely to be the case), then the area of each nanoparticle will approximately be the height squared. This gives $(2.4\ \text{nm})^2 = 5.8\ \text{nm}^2$ and $(4.2\ \text{nm})^2 = 17.6\ \text{nm}^2$, respectively. These numbers are rather close to the average nanodot sizes of 7.5 and 20.0 nm^2 found from the SEM analysis (see Table 2).

Results from a similar analysis of the Au layers deposited on ZnO are also shown in Table 2. The XPS analysis for 1.5 nm on ZnO is shown in parenthesis because it is uncertain due to the presence of Ag peaks originating from the silver paste in the XPS spectrum for this sample.

Concerning the gold coverage of the transparent conductive anodes, the agreement of the results obtained by the two different methods is excellent since both techniques give similar coverage and island height values. Moreover, these results are also in good agreement with works reported earlier since a coverage of about 80–90% has been measured by time of flight secondary ion mass spectroscopy analysis for 4-nm-thick gold films [4]. It can be seen that for the optimal Au thickness with regard to the performance of OPV cells, obtained with nominal 0.5-nm Au, only about 15% of the ITO or ZnO is covered with Au. However, these gold nanodots have shown a very efficient behaviour as an anode buffer layer. This means that if in the case of PEDOT:PSS the buffer layer should cover the whole surface of the ITO or ZnO film, in the case of gold, a coverage of only 15% is enough to be active as a buffer layer, which shows that gold is very efficient as an anode buffer layer in OPV cells, which means that this ultrathin film tailors the anode work function efficiently.

Conclusions

The use of the open-source software ImageJ for SEM analysis and of the QUASES-Tougaard method for the analysis of XPS is a valuable support for a scientific estimation of surface coverage and nanodot height since we found an excellent agreement between the results of both techniques. The analysis of the shape of the inelastic XPS

peak and the surface coverage estimation through the SEM image treatment gave similar results. From the values obtained from these two techniques, we can conclude that Au is a very efficient anode buffer layer since a coverage of only ~15% of the ITO anode is sufficient to achieve results similar to those obtained with a continuous PEDOT:PSS buffer layer.

References

1. Bernède JC, Godoy A, Cattin L, Diaz FR, Morsli M, del Valle MA (2010) Organic solar cells performances improvement induced by interface buffer layers. In: Rugescu RD (ed) Solar energy. Intech-Vukovar, Croatia. ISBN 978-953-307-052-0
2. Godoy A, Cattin L, Toumi L, Diaz FR, del Valle MA, Soto GM, Kouskoussa B, Morsli M, Benchouk K, Khelil A, Bernède JC (2010) Sol Energy Mater Sol Cells 94:648–654
3. Schulze K, Uhrich C, Schüppel R, Léo K, Pfeiffer M, Brier E, Reinold E, Bäuerle P (2006) Adv Mater 18:2872–2875
4. Hatton RA, Willis MR, Chesters MA, Rutten FJM, Briggs D (2003) J Mater Chem 13:38–43
5. Tadayyon SM, Griffiths K, Norton PR, Tripp C, Popovic Z, Vac J (1999) Sci Technol A 17:1773–1778
6. Bernède JC, Cattin L, Morsli M, Berredjem Y (2008) Sol Energy Mater Sol Cells 92:1508–1515
7. Bernède JC, Berredjem Y, Cattin L, Morsli M (2008) Appl Phys Lett 92:083304
8. Peumans P, Bulovic V, Forrest SR (2000) Appl Phys Lett 76:2650–2652
9. Latef A, Bernède JC (1991) Phys Status Solidi A 124:243–252
10. Papadopulos F, Spinelli M, Valente S, Foroni L, Orrico C, Alviano F, Pasquinelli G (2007) Ultrastruct Pathol 31:401–407
11. Tougaard S (1998) Surf Interface Anal 26:249–269
12. Tougaard S, Electron J (2010) Spectrosc Relat Phenom 178:128–153
13. Winters HF, Graves DB, Humbird D, Tougaard S, Vac J (2007) Sci Technol A 25:96–103
14. Preda I, Soriano L, Alvarez L, Méndez J, Yubero F, Gutiérrez A, Sanz JM (2010) Surf Interface Anal 42:869–873
15. Tougaard S. QUASES-Tougaard Ver. 5.3 (1994–2010). Software for quantitative XPS/AES of surface nanostructures by analysis of the XPS peak–intensity and background shape. www.quases.com